

Article

# Combined Effect of Photocatalyst, Superplasticizer, and Glass Fiber on the Photocatalytic Activity and Technical Parameters of Gypsum

Kamila Zajac<sup>1</sup>, Adam Czyzewski<sup>2</sup>, Maria Kaszyńska<sup>1</sup> and Magdalena Janus<sup>1,\*</sup> 

<sup>1</sup> Faculty of Civil Engineering and Architecture, West Pomeranian University of Technology, Szczecin, al. Piastów 50, 70-311 Szczecin, Poland; kamila.zajac@zut.edu.pl (K.Z.); maria.kaszynska@zut.edu.pl (M.K.)

<sup>2</sup> Faculty of Chemical Technology and Engineering, West Pomeranian University of Technology, Szczecin, ul. Pułaskiego 10, 70-322 Szczecin, Poland; adam.czyzewski@zut.edu.pl

\* Correspondence: magdalena.janus@zut.edu.pl; Tel.: +48-91-449-4083

Received: 12 March 2020; Accepted: 31 March 2020; Published: 1 April 2020



**Abstract:** In this study, gypsum plasters enriched with the modified photocatalyst TiO<sub>2</sub>/N and additive components were prepared and analyzed in detail. The aim of this work was to recognize the combined impact of a photocatalyst, polycarboxylic superplasticizer (SP), and glass fiber (F) on the properties of the composed building materials. The mutual compatibility was verified in relation to self-cleaning and air-purifying activity as well as to the technical parameters defined in standards for gypsum materials. The measurements revealed that photocatalytic gypsum material can have high mechanical strength and limited shrinkage as a result of superplasticizer contribution in form of a water-reducing and well-dispersive agent. Normal consistency was achieved by the addition of 0.01 wt % of SP to photocatalytic gypsum mortar or by the addition of 0.2 wt % of SP with a 12% reduction of water. This study also explains why glass fiber fulfills the role of inner reinforcement only if a superplasticizer is simultaneously added to the gypsum matrix. It is possible, by the combined effect of TiO<sub>2</sub>/N, a polycarboxylic superplasticizer, and glass fiber, to achieve NO<sub>x</sub> degradation at a high level. Moreover, the significantly improved self-cleaning properties of the complex gypsum plasters surfaces from dye pollutants in comparison to a gypsum plaster with solely a TiO<sub>2</sub>/N photocatalyst indicate the synergistic effect of the three considered additives.

**Keywords:** titanium dioxide; photocatalytic building materials; gypsum plaster; self-cleaning properties

## 1. Introduction

Advanced building materials using heterogeneous photocatalysis have attracted increasing attention for de-polluting air, material self-cleaning, inactivating bacteria, and preventing algae growth [1]. Photocatalyst nanoparticles, especially TiO<sub>2</sub>, are incorporated into building material mass or immobilized onto building material surfaces [2]. In the photocatalytic way, many harmful pollutants might be degraded into small nontoxic inorganic molecules (such as H<sub>2</sub>O and CO<sub>2</sub>) [3], whereas photocatalytic action is necessary only for UV irradiation, humidity, and the initial adsorption of the pollutants molecules on the photocatalyst surface [4]. Up to now, cement and concrete materials have been intensively studied regarding the impact of TiO<sub>2</sub> photocatalyst particles on the activity properties and technical parameters of the final building products [5]. The promising potential of the photocatalytic cement materials was confirmed both in experimental setups and on construction sites, for example, the ‘Dives in Misericordia’ church in Rome (Italy) and ‘l’Ecole de Musique’ in Chambéry (France) [6]. However, the development of modified types of TiO<sub>2</sub> and the extension of an activation spectrum for visible light [7] makes it reasonable to focus on building materials dedicated to interiors of buildings, such as gypsum materials.

One of the problems with photocatalytic additives is that the powder particles tend to reduce the amount of free water in the building mixtures. More water is required to wet and wrap the surface of TiO<sub>2</sub> particles due to their extremely fine size and high specific surface area. On the one hand, it causes a decrease in the fluidity of building mortars and consequently a decline in the workability. On the other hand, it can lead to an increase in the water demand in building mortars for obtaining similar flowability as in mortars without photocatalyst particles. However, the higher water amount might result in an increase in porosity and loss of mechanical properties [8–10].

We reported in our previous research [11] that glass fiber is a very effective way to improve the self-cleaning properties of gypsum plaster. It was found that through simultaneously using photocatalyst particles and glass fiber in gypsum plaster, the photocatalytic activity was about two times higher than that of an adequate sample without glass fiber. The photocatalytic action of glass fiber was excluded. It was clearly demonstrated that the enhancing self-cleaning effect in the presence of glass fiber resulted from the other phenomena. Namely, glass fiber may act as ducts for irradiation to deeper parts of building material and transport the light to TiO<sub>2</sub> sites screened by other particles or enhance the charge separation. We have displayed that using 1 wt % of the modified photocatalyst TiO<sub>2</sub>/N and glass fiber in gypsum plaster allowed obtaining nearly 10% better efficiency than using 3 wt % of the same TiO<sub>2</sub>/N without glass fiber, respectively 57% versus 48% for Reactive Orange 20 degradation. The modification of the base structure of TiO<sub>2</sub> by a nitrogen element involved the visible response of the photocatalyst, which has been widely described in the literature [12,13]. Based on our previous studies [11], the glass fiber appeared to be effective for the transmission of the both sources of irradiation. Thereby, under UV as well as visible light, the degradation rate was higher, when the gypsum matrix apart from TiO<sub>2</sub>/N also glass fiber was used.

However, the initial intention of glass fiber incorporation into gypsum plaster was the inner reinforcement of the material. Despite the excellent photocatalytic performance of the above-described gypsum composites, we observed from the synthesized samples that the glass fiber was not as effective as expected in mechanical strength enhancement. Therefore, to solve the problem, and in order to improve the mechanical parameters of the modified gypsum plaster, other additives might be taken into account, for example, the coupling of photocatalytic gypsum plaster with a superplasticizer.

Superplasticizers influence the rheological properties of fresh mortars [14]. Generally, superplasticizers promote the consistency and workability of concrete under the same water/binder ratio or are capable of reducing water content, up to 30%, maintaining the same consistency [15]. Some of the most common types of superplasticizers used are either based on lignosulfonate or polycarboxylic compounds [16]. The advantage of the second is their high capacity at low dosages [17]. The better dispersion of grains using polycarboxylic-based superplasticizers resulted mainly from a mechanism called steric hindrance as well as partly from electrostatic repulsion (from the negatively charged carboxylic groups) and lubricating action [18].

Some authors demonstrated that the effect of superplasticizer on building materials performance is dependent on the type and dosage of superplasticizer as well as the type of binder [19]. The main binder studied in conjunction with superplasticizer is cement, whereas reports about the coupled effect of superplasticizer with gypsum are rather scarce. However, Tan et al. [20] indicated that polycarboxylic superplasticizer, as the most efficient dispersant in cement-based materials, also shows a good ability to disperse the gypsum particles. Peng et al. [21] compared the effects of two types of superplasticizer on gypsum plaster:  $\beta$ -naphthalene sulfonic acid type and polycarboxylate type. It appeared that the first case belonged to physical adsorption, whereas the polycarboxylic molecules were adsorbed on gypsum in the form of chemisorption; the small adsorption amount and the good dispersion stability were confirmed. The results of other authors [22–24] showed that the addition of superplasticizer to gypsum-based material gives a dense and well-compacted structure of gypsum crystals, leading to higher strengths in the hardened materials and better water resistance for the gypsum matrix.

In this study, polycarboxylic superplasticizer (SP) was added to the gypsum matrix. We considered the incorporation of the three additives—TiO<sub>2</sub>/N photocatalyst, glass fiber (F), and superplasticizer—as

the modifying agents in gypsum plaster. The as-prepared composites were characterized toward technical parameters: consistency, setting time, shrinkage, flexural strength, and compressive strength; special attention was also paid to self-cleaning properties (RE) and the ability to purify air.

## 2. Results and Discussion

### 2.1. Consistency

The water demand for commercial gypsum plaster (G) in Table 1 was determined. The normal consistency for the gypsum plasters (according to PN-EN 13279-2) is achieved when the spread diameter is in range of 15–21 cm. The accepted consistency of G sample was obtained for a water/plaster ratio (W/P) of 0.85. The addition of 1 wt % TiO<sub>2</sub>/N photocatalyst to gypsum matrix (PG) involved a higher water demand of the obtained mixture. It was proved in our previous work [25] that the increasing additive of TiO<sub>2</sub>/N photocatalyst to the gypsum matrix (from 1 wt % to 5 wt % of plaster mass) caused a successive reduction of spread diameter. It showed that the mortar continued getting thicker with the higher photocatalyst content. In the case of the PG sample, the consistency was comparable with G mortar when the W/P ratio was increased to 0.87.

**Table 1.** Water demand for the normal consistency of gypsum plaster and photocatalytic gypsum plaster. G: commercial gypsum plaster, PG: addition of 1 wt % TiO<sub>2</sub>/N photocatalyst to gypsum matrix, PG-SP1: superplasticizer in photocatalytic gypsum plaster, SP: superplasticizer, W/P: water/plaster ratio.

| Sample | SP Dose (wt. %) | W/P Ratio | Average Spread Diameter with Standard Deviations (cm) |
|--------|-----------------|-----------|---|
| G      | -               | 0.67      | 10.0  |
|        |                 | 0.80      | 13.0  |
|        |                 | 0.85      | 14.5 ± 0.1  |
| PG     | -               | 0.85      | 13.8 ± 0.2  |
|        |                 | 0.88      | 15.1 ± 0.1  |
|        |                 | 0.87      | 14.6 ± 0.1  |
| PG-SP1 | 0.50            | 0.85      | 16.6 ± 0.1  |
|        | 0.20            | 0.85      | 16.0  |
|        | 0.10            | 0.85      | 16.0  |
|        | 0.05            | 0.85      | 15.9 ± 0.1  |
|        | 0.01            | 0.85      | 14.7 ± 0.2  |

To illustrate how the consistency of photocatalytic gypsum plaster varied with SP dosage, the spread diameter results in Table 1 are gathered. The presence of SP in photocatalytic gypsum plaster (PG-SP1) improved its flowability using the constant water content (W/P = 0.85). However, scarcely 0.01 wt % of SP in photocatalytic mortar was efficient enough to obtain the comparable consistency with the G sample.

In the next series of the experiment, the reduction of water in photocatalytic plasters was carried out. The W/P ratio decreased from 0.85 to 0.75, and different doses of SP were added to obtain an acceptable consistency (Table 2). The assortment of SP doses in photocatalytic gypsum mortar was carried out by the trial and error method beginning from 0.1 wt % of SP in photocatalytic plaster and varying the subsequent SP dose of 0.05 wt % (e.g., 0.15 wt %, 0.20 wt %). It can be observed that the application of SP allowed reducing the water content in photocatalytic gypsum mortar (PG-SP2). Comparing the respective spread diameter results using W/P = 0.75, it is evident that 0.2 wt % of SP in photocatalytic mortar led to achieving the desired consistency. It should be mentioned that the reduction of 12% water (corresponding to a W/P decrease from 0.85 to 0.75) caused the decrease of flowability of the reference gypsum mortar in an unaccepted range, which is connected with its lower workability.

**Table 2.** Assortment of SP dose in photocatalytic gypsum plaster: the reduction of water content.

| Sample | SP Dose (wt.%) | W/P Ratio | Average Spread Diameter with Standard Deviations (cm) |
|--------|----------------|-----------|---|
| G      | -              | 0.75      | 12.0  |
| PG     | -              | 0.75      | 11.3  |
| PG-SP2 | 0.10           | 0.75      | 14.1 ± 0.1  |
|        | 0.15           | 0.75      | 14.2 ± 0.1  |
|        | 0.20           | 0.75      | 14.4 ± 0.1  |

In order to make further detailed analyses, the gypsum mortars that had comparable consistency were selected. The five gypsum samples showed the consistency oscillating the lower limit of the normal consistency (spread diameter about 15 cm). Their precise compositions were presented in Table 3. Some of them were obtained with the initial W/P ratio = 0.85 (G, PG, and PG-SP1) and some of them were obtained with the lower W/P ratio = 0.75 (PG-SP2 and PG-SP2-F). In PG mortar, the W/P ratio was set at 0.85 in order to assure the comparable water content between the following mortars: G, PG, and PG-SP1. The reduction of W/P = 0.87 to 0.85 for PG did not cause a noticeable loss of workability. The selection of the indicated mortars allowed considering the SP function in both ways. The SP presence in the photocatalytic gypsum matrix was studied as a function of the improvement of flowability (PG-SP1) as well as its role in reducing the water demand (PG-SP2). Moreover, the simultaneous use of glass fiber in the photocatalytic gypsum mortar was tested (PG-SP2-F).

**Table 3.** Compositional data for the selected gypsum plasters.

| Sample   | TiO <sub>2</sub> /N Dose (wt.%) | SP Dose (wt.%) | F Dose (wt.%) | W/P Ratio |
|----------|---------------------------------|----------------|---------------|-----------|
| G        | 0.00                            | 0.00           | 0.00          | 0.85      |
| PG       | 1.00                            | 0.00           | 0.00          | 0.85      |
| PG-SP1   | 1.00                            | 0.01           | 0.00          | 0.85      |
| PG-SP2   | 1.00                            | 0.20           | 0.00          | 0.75      |
| PG-SP2-F | 1.00                            | 0.20           | 0.30          | 0.75      |

## 2.2. Setting Time

The initial setting time of gypsum mortars was measured as a period between the moment of adding the plaster with gypsum hemihydrates to the water and the time when the cone immersed in the test block and did not reach the bottom of the mold, which was about 22 ± 2 mm above the bottom. The added TiO<sub>2</sub>/N influenced the initial setting time of the modified gypsum plaster, which was illustrated in Figure 1. It appeared that 1 wt % of the photocatalyst in plaster mass resulted in a 30 min shorter setting time. Referring to the theory [26,27], the setting of plaster is the hydration process, which occurs through the crystallization mechanism. The transformation of gypsum binders into a solid body happens gradually. Calcium sulfate hemihydrate dissolves in water and then the calcium sulfate dihydrate (gypsum) precipitates from the aqueous solution. It was found [28] that titanium dioxide can act as a catalyst for the hydration reaction. In photocatalytic cements, the particles of TiO<sub>2</sub> photocatalyst played the role of centers of nucleation and the accumulation of hydration products. Thus, the kinetics of the hydration reaction and hence the setting time of modified gypsum plasters can be also changed.

The small amount of SP (0.01 wt %) in photocatalytic plaster (PG-SP1) did not influence the setting time. However, with the addition of 0.2 wt % of SP (PG-SP2), an acceleration of setting time over the next 40 minutes was observed. On the one hand, in samples at W/P = 0.75, the excess of water to remove was lower and the curing of gypsum might proceed faster. On the other hand, the polycarboxylic SP is designed to assure effective dispersion without blocking the hydration process. Namely, the side chains

of the main SP molecule separate the plaster grains and increase their access area for water. Then, they facilitate the hydration; thus, the setting time might be shortened. In spite of the acceleration effect, the modified plasters fulfilled standard requirements (setting time >50 min).

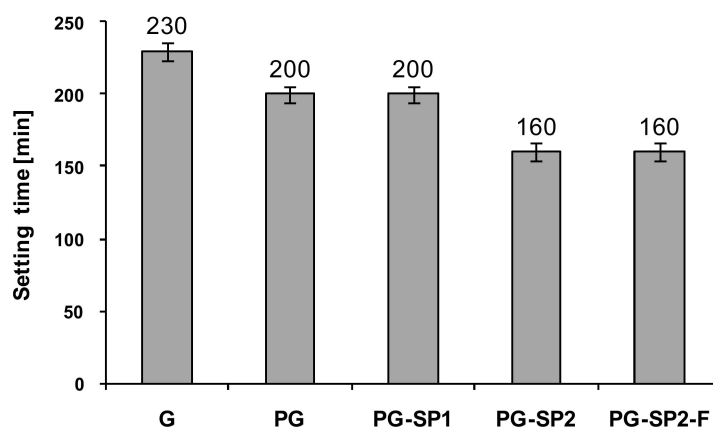


**Figure 1.** The initial setting time of modified gypsum plasters with standard deviations.

### 2.3. Mechanical Properties

The changes of mechanical strength in modified gypsum plasters in Figure 2 were plotted. The reference gypsum matrix is in accordance with standards. Namely, the flexural and compressive strengths of gypsum plaster should not be lower than 1 MPa and 2 MPa, respectively (PN-EN 13279-2). Meanwhile, the addition of 1 wt % of TiO<sub>2</sub>/N to starting gypsum plaster involved a significant decrease of mechanical properties. The flexural strength of PG was lower by about 20% as compared to the control sample (Figure 2a), and the compressive strength decreased by about 22% (Figure 2b), whereas the water content in G and PG mortars was the same. It is worth mentioning that at the same consistency (W/P = 0.85 for G and W/P = 0.87 for PG), the declines were even higher, about 25% and 37%, respectively for flexural and compressive strength. While it was expected to have lower strengths with higher water content, the results with the same W/P ratio = 0.85 for G and PG indicated the influence of photocatalyst particles on the gypsum matrix. The observation could be attributable to changes in the mortar microstructure, pore size, and distribution, which were reported by Lucas et al. [29] in similar studies. The authors showed that among various building materials, such as cement, lime, and gypsum, the influence of TiO<sub>2</sub> addition (commercial form) on mechanical strength loss was the highest in the case of gypsum binders. They explained that after the addition of photocatalyst to the gypsum matrix, the pore size reduction is significant (<10 μm) but not sufficient to prevent the mechanical strength decrease. On the contrary, in cement mortars, the combined effect of photocatalyst presence was observed. Namely, the lower content of macropores (>10 μm) and higher amount of nanopores (<1 μm) are able to stabilize the mechanical strength or even enhance it.

The small amount of SP (0.01 wt %) in photocatalytic plaster (PG-SP1) improved the flexural strength (6%) slightly. However, the dose of 0.2 wt % of SP connected with a simultaneous 12% reduction of water (PG-SP2) contributed to a significant enhancement in the mechanical strength of photocatalytic gypsum plasters. According to Figure 2, both the flexural and compressive strengths increased by respectively 77% and 68%. Moreover, the modified PG-SP2 mortar appeared to have better mechanical parameters than the reference G mortar; the flexural strength increased by 42% and compressive strength was about 32% higher. Primarily, the observed enhancement is a result of the lower water content in the gypsum matrix. The positive SP effect on the mechanical strength can be also attributed to the side chains of the main SP molecule, which improve the dispersion of plaster components and prevent the creation of big irregular agglomerates. Moreover, the water molecules, which could be occlusive in the aggregates, are accessible, and its better use for wetting

the grains is ensured. Pundir et al. [23] indicated that the high strength of gypsum samples after the application of superplasticizer is connected with the formation of a dense and well-compacted texture of crystals, and the role of superplasticizer molecules as a kind of cross-linking agent, which increases the intercrystalline bonding between the crystals of gypsum. However, it was also reported [30] that polycarboxylic superplasticizer decelerates the early hydration of gypsum. Superplasticizing molecules can adsorb on the building materials grains in excess, which involves limited water access at the beginning of the hydration process [31].

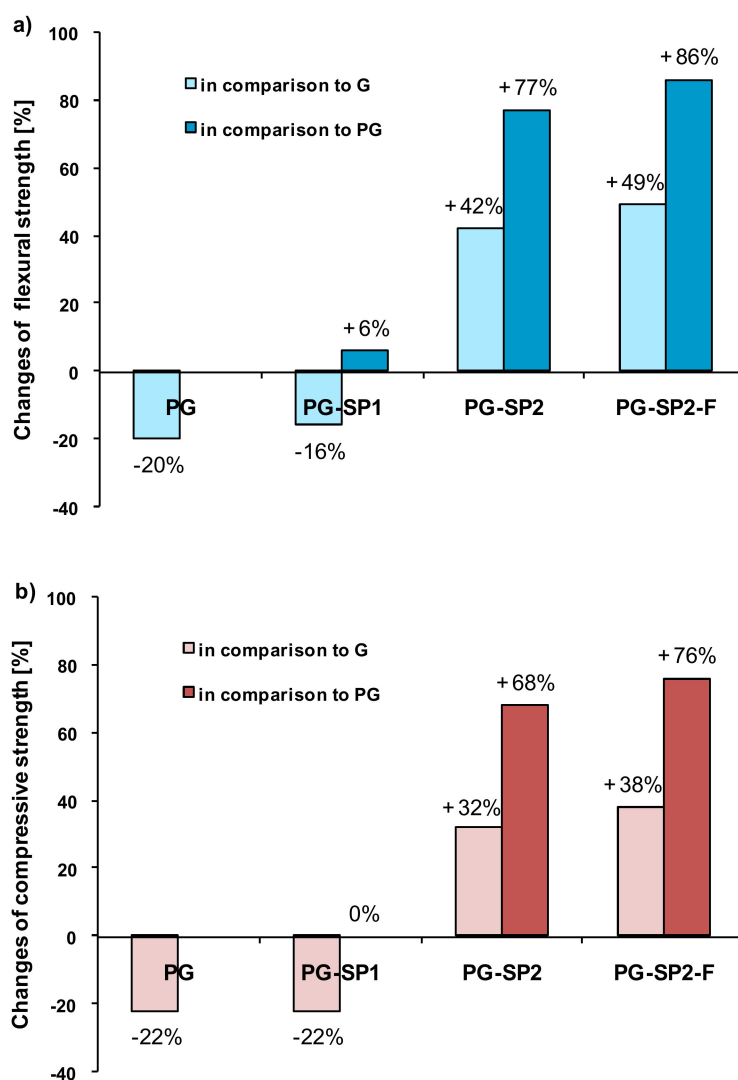


**Figure 2.** The changes in the mechanical properties of modified gypsum plasters: (a) flexural strength; (b) compressive strength.

Contrasting our previous results [11], in the current samples, the glass fiber induced the enhanced resistance of photocatalytic gypsum materials to mechanical forces. The only difference between the PG-SP2 and PG-SP2-F mortars is the presence of glass fiber in the second one. The mutual comparison of the two samples shows that the glass fiber led to 9% and 8% higher mechanical strength, respectively for flexural and compressive forces. It seems that what is essential in the effective affection of glass reinforcement is the concurrent SP presence in photocatalytic gypsum plasters. Huang recommended in his work [32] that fiber should always be accompanied by the incorporation of a superplasticizer to assure improved physical properties of building materials. He presented cement substituted by fly ash in 30% and containing organic fiber and superplasticizer. The addition of fiber alone into

cement–fly ash material resulted in a slight reduction of compressive strength. It was attributed to the redistribution of the void structure due to the fiber inclusion and weak interfacial bonds between the fiber and grains of the building material. However, the addition of superplasticizer beside the fiber allowed correcting the adverse fiber affection through the formation of a well-dispersed homogeneous structure of the modified mortar.

#### 2.4. Shrinkage

The results of shrinkage tests for modified gypsum plasters are presented in Figure 3. All of the measurements were conducted after demolding of the samples; thereby, they describe the drying shrinkage. Among three specimens of each samples, in most cases, the standard deviation did not exceed 0.01 mm/m. In the first day after demolding, the lowest change of length was observed in the case of photocatalytic plaster PG ( $-0.07$  mm/m). For the other four mortars, the shrinkage was varied in the first phase of drying. From the fifth to 10th day of mortars, curing proceeded the successive increase of shrinkage in nearly all samples. After 10 days, the stabilization of shrinkage succeeded. Comparison of the final shrinkage values between the respective modified plasters was performed after 28 days of curing.

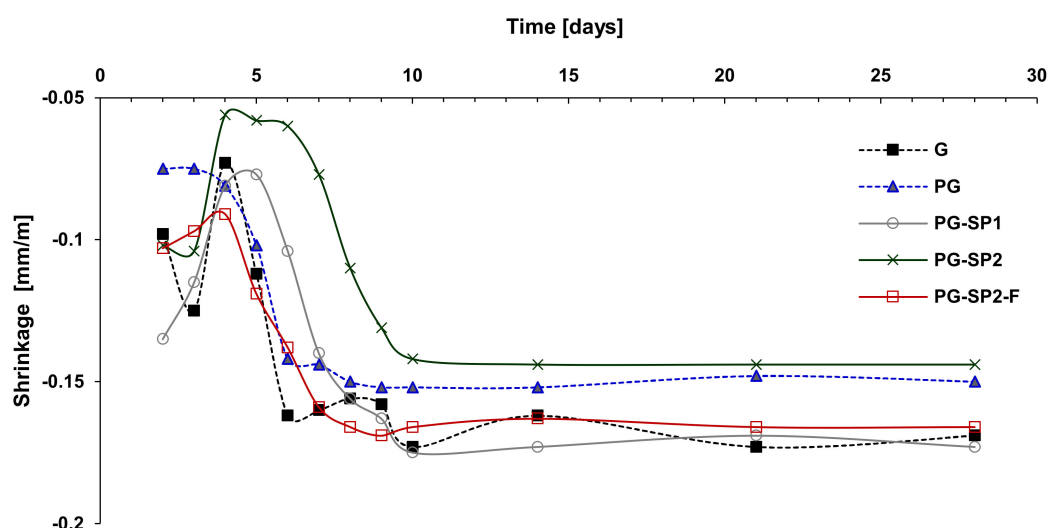


Figure 3. The shrinkage of modified gypsum plasters during 28 days of curing.

The shrinkage of gypsum plaster with 1 wt % of  $\text{TiO}_2/\text{N}$  (PG) was on the level of ( $-0.150$  mm/m), which gives a shrinkage reduction of 11% in relation to the reference gypsum plaster G ( $-0.169$  mm/m). The nanometric photocatalyst probably influences the microstructure of plasters, which affects the course of shrinkage changes. Farzдания et al. [33] registered that the inclusion of nanosilica into cement mortars limited the drying shrinkage rate. They connected the results with the reduction of total porosity and the filling effect by nanoparticles in building matrix. A similar impact on the reduction of shrinkage was in the case of photocatalyst particles in the gypsum matrix. The nanosized photocatalyst particles, which fill the areas between the grains of the building material, can compensate for the decrease of water in the material during the drying process.

The greatest reduction of shrinkage was observed for gypsum plaster modified by both the photocatalyst and superplasticizer, with the simultaneous reduction of water content (PG-SP2). The curve of the PG-SP2 in the timeline showed the lowest changes of sample length in comparison to the curves of other samples. Consequently, the shrinkage was reduced by about 15% in relation to the unmodified sample ( $-0.144$  mm/m for PG-SP2 versus  $-0.169$  mm/m for G). The combined effect of nanometric or micrometric material and superplasticizer on building materials was also observed by other authors [34,35]. Sonebi et al. [34] registered that the increasing nanosilica content in cement

mortars (from 0.5 wt % to 3.5 wt %) significantly reduced plastic shrinkage from about 2% to 1%. However, the simultaneous increasing superplasticizer content (from 0.3 wt % to 0.9 wt %) gave the increased shrinkage from about 2% to 3%. Alasyed [35] indicated that the silica fume addition allowed reducing the sensitivity of concrete to the curing conditions. The inclusion of silica fume (10% of cement weight) in the concrete mix decreased the drying shrinkage by 25%, whereas the combined effect of silica fume and plasticizer or superplasticizer may contribute to an increase of the shrinkage rate.

It seems that the analogous contrary action of photocatalyst and superplasticizer was observed in our work. Namely, the dope of photocatalyst into the gypsum matrix reduced the shrinkage (PG), whereas the contemporaneous low dose of superplasticizer eliminated the reduction (PG-SP1). However, the reduction of water in gypsum mortar, as a result of the higher amount of superplasticizer accompanying the presence of photocatalyst in gypsum mortar, allowed obtaining the highest reduction of shrinkage. It indicates the significance of water reduction in the limitation of volume and length changes of samples during the drying process rather than the direct effect of superplasticizer presence in the gypsum matrix.

In the case of the sample with glass fiber (PG-SP2-F), the rate of shrinkage was comparable to the results for the reference G plaster. Several studies have evaluated the shrinkage and cracking behavior of building materials with fiber reinforcement [36,37]. Hwang [36] reported that adding coconut fiber into building composites reduced cracking, which is attributable to the shrinkage effect. The major reason for this phenomenon was connected with the fact that fibers facilitate the bridging of cracks in the mortars. However, in our sample, the bridging effect was not observed, which was probably due to the character of the fiber surface. The glass fiber appeared to be smooth without remarkable roughness, which favors the skidding effect and the limitation of rubbing. Thereby, the glass fiber did not inhibit the move of the matrix during the drying of the matrix. The mortar could freely relocate within the surface of the fiber in the process of curing.

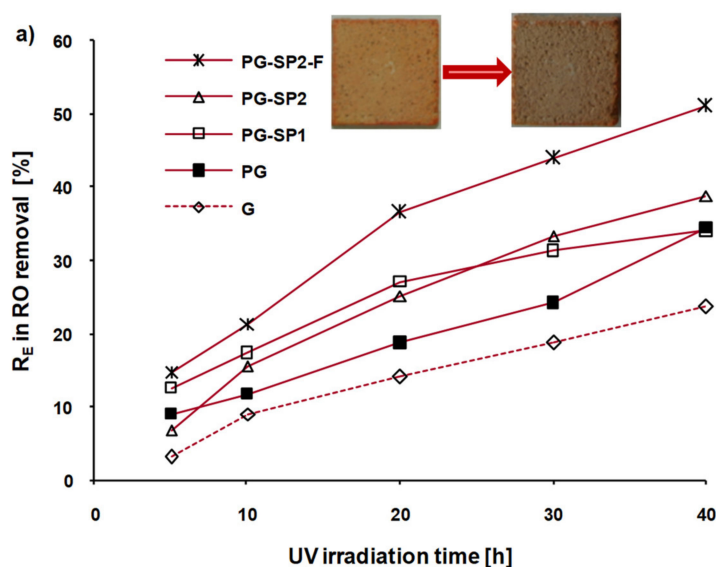
### 2.5. Photocatalytic Activity

The photocatalytic performance of the prepared gypsum plasters toward  $\text{NO}_x$  degradation is depicted in Table 4. It can be clearly observed that  $\text{TiO}_2/\text{N}$  presence in the gypsum matrix involved the significant decrease of  $\text{NO}_x$  concentration (31%). It should be stressed that the reference G sample did not show any properties to remove the model pollutant from air; in addition, the experiments with PG in dark conditions excluded other effects than the photocatalysis process. It appeared a concern that the direct contact of photocatalyst with a superplasticizer in the gypsum matrix might involve the photocatalytic degradation of the SP molecules under irradiation. Admittedly, the role of SP is fulfilled at the beginning of the process during the mixing operation, but SP molecules could compete with model pollutants for active sites on the photocatalyst surface. The results showed that the potential degradation of SP molecules did not interfere with both the photocatalytic activity and technical parameters. Gypsum plasters containing a superplasticizer beside the photocatalyst in the matrix showed the maintenance of the  $\text{NO}_x$  degradation rate. The application of a lower SP dose (0.01 wt %) or the higher SP loading (0.2 wt %) as well as the glass fiber simultaneously in the gypsum matrix allowed obtaining  $\text{NO}_x$  reduction at the level of about 30%. Moreover, the additional components (SP, F) seemed to influence slightly on the selectivity in reference to the production of  $\text{NO}_2$  with respect to the total number of converted NO particles. Namely, using the PG-SP1, PG-SP2, and PG-SP2-F samples, the temporary concentration of  $\text{NO}_2$  is lower than in the case of PG.  $\text{NO}_2$ , as a first intermediate in the photocatalytic conversion of NO, is significantly more toxic than NO. Hence, the more efficient plasters are those that attain a higher selectivity of NO to  $\text{NO}_3^-$  than NO to  $\text{NO}_2$ , which was attributed to the gypsum samples with SP.

**Table 4.** Activity of modified gypsum plasters toward NO<sub>x</sub> degradation.

| Sample   | NO Removal (μg/cm <sup>2</sup> /h) | NO <sub>2</sub> Formation (μg/cm <sup>2</sup> /h) | NO <sub>x</sub> Total Removal (μg/cm <sup>2</sup> /h) | Rate of NO <sub>x</sub> Degradation with Standard Deviations (%) |
|----------|------------------------------------|---|---|--|
| G        | 1.18                               | 0.00  | 1.18  | 2.4 ± 0.5  |
| PG       | 11.67                              | 1.47  | 10.20   | 31.0 ± 2.0   |
| PG-SP1   | 12.48                              | 1.39  | 11.09   | 33.4 ± 1.0   |
| PG-SP2   | 10.95                              | 1.20  | 9.75  | 29.4 ± 2.0   |
| PG-SP2-F | 12.31                              | 1.15  | 11.16   | 33.3 ± 2.0   |

The self-cleaning effects (RE) of modified gypsum plasters are illustrated in Figure 4 during the degradation of Reactive Orange 20 (RO) and Malachite Green (MG) dyes. It ought to be stressed that the standard deviations never exceeded 3%. Therefore, in the plotted results, only mean values are presented. In comparison to the simple bleaching of dyes on the G surface, the PG sample showed photocatalytic properties. The self-cleaning action was maintained using SP in the photocatalytic gypsum matrix. The dye's degradation rate was even improved on the surface of PG-SP2 in reference to PG after 40 h of UV irradiation from 34% to 39% for RO and from 33% to 38% for MG. It can be explained by the better dispersion of individual components of plaster as a result of SP presence. The limited agglomeration of TiO<sub>2</sub>/N particles ensured higher accessibility to the active surface of the photocatalyst. It appeared that the effect of glass fiber in photocatalytic gypsum mortar was the same as it was reported previously [11], regardless of SP presence. The self-cleaning efficiency of PG-SP2-F toward RO degradation amounted to 51% within 40 h of UV irradiation, which was nearly 2 times higher than the correspondence results of PG plaster. The cationic dye—MG in comparison to the anionic dye—RO, was removed to a minor extent from the surface of modified gypsum plasters. However, in the case of MG, the enhancement of the self-cleaning effect with the contemporaneous presence of photocatalyst TiO<sub>2</sub>/N, SP, and glass fiber in comparison to gypsum plaster with only photocatalyst was also observed (after 40 h of UV 41% versus 33%). Typically, it is difficult for any photocatalyst to degrade both anionic and cationic compounds with equal simplicity [38].

**Figure 4.** Cont.

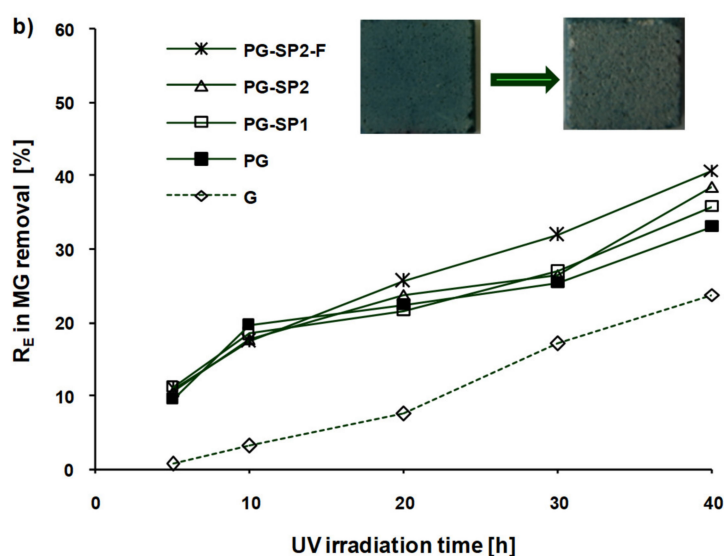


**Figure 4.** Self-cleaning properties of modified gypsum plasters as a function of UV irradiation time: (a) degradation of Reactive Orange 20; (b) degradation of Malachite Green.

### 3. Materials and Methods

#### 3.1. Materials

Commercial gypsum plaster (Knauf MP75, Iphofen, Germany) was used as a gypsum matrix. The modified  $\text{TiO}_2/\text{N}$  was used as a photocatalyst. The  $\text{TiO}_2/\text{N}$  photocatalyst was synthesized from commercial amorphous titania (GrupaAzotyZakładyChemiczne "Police" S.A., Poland) and diluted ammonia water (2.5 wt %, Chempur, Poland) using HEL Ltd. Autolab E746 installation (HEL Ltd., Borehamwood, UK). The detailed procedure was described in our previous works [39,40]. In short, the role of modification was an insertion of nitrogen into the structure of starting titania, which was carried out in the liquid phase at 100 °C and autogenous pressure. Then, the obtained slurry was heated at 100 °C and grounded to form a fine powder. The final  $\text{TiO}_2/\text{N}$  has a surface area of 235  $\text{m}^2/\text{g}$  according to the BET method, a crystallite size of about 12 nm according to X-ray powder diffraction (XRD), and the participation of crystalline phases is 97% and 3%, respectively for anatase and rutile. Nitrogen presence in titania was confirmed by Fourier transform infrared spectroscopy (FTIR) and amounted to 0.49 wt % according to ONH 836 Oxygen/Nitrogen/Hydrogen analyzer (Leco, USA) [25,39].

A polycarboxylate-based superplasticizer, MasterGlenium ACE 430 (SP), was used as a modern superplasticizing agent, which was supplied by the Master Builders company. The glass fiber (F) was used as a dispersed reinforcement (type E, Rozenblat company, Mosian, Poland). This aluminosilicate glass was in form of fibers chopped to a length of 12 mm. Gaseous NO (1.989 ppm  $\pm$  0.040 ppm, Air Liquid), Reactive Orange 20—RO, and Malachite Green—MG (Boruta-Kolor Sp. z o.o., Poland) were used as model organic pollutants.

#### 3.2. Preparation of Gypsum Samples

Gypsum samples were prepared to determine the technical and photocatalytic properties of the modified plasters. Different compositions of the samples were compiled in order to understand the effect of various additives. The starting gypsum plaster was used as the reference material (G). The modified samples were prepared by adding  $\text{TiO}_2/\text{N}$  photocatalyst (1 wt %) and/or superplasticizer in a dosage range of 0.01–0.20 wt % and/or glass fiber in amount of 0.3 wt % to the gypsum plaster. Briefly, the starting gypsum plaster was mixed with  $\text{TiO}_2/\text{N}$  photocatalyst. The homogeneous powder was slowly transferred into the mixing bowl containing water. Prior to the mixing with water, it was allowed to soak the water into the powder mass for about a minute. The ratios of water to plaster

(W/P) were determined during the studies. The superplasticizer and/or glass fiber were added at the end of mixing with water. Immediately after mixing, the obtained pastes were cast into silicone molds. The specimens of size  $40 \times 40 \times 160$  mm (for flexural strength and shrinkage) and  $20 \times 20 \times 6$  mm (for photocatalytic activity) were setting at  $20 \pm 2$  °C. After final setting, the gypsum samples were removed from molds. In the case of analyses referring to the mechanical strength and photocatalytic properties, each specimen was dried to a constant weight at 40 °C and cooled to room temperature. In contrast, the samples intended for shrinkage analysis were measured directly after demolding.

### 3.3. Measurements of Technical Parameters

The consistency, setting time, and mechanical strength of modified gypsum plasters were tested in accordance with the PN-EN 13279-2 Standard: “Gypsum binders and gypsum plasters. Part 2: Test methods”. The consistency was studied by the dispersion method. After the removal of Vicat’s ring, the spread diameter of mortars was measured. The setting time was studied using a Vicat’s apparatus equipped with an immersion cone. The flexural and compressive strengths were tested using a Water + Bai machine, OB 3000/200 (Switzerland). The prepared specimens were first subjected to a flexural strength test. Then, the compressive strength was tested on halves of broken specimens. The shrinkage of the modified gypsum samples was analyzed using the Graf-Kaufman method and an appropriate Graf-Kaufman apparatus. During the shrinkage measurements, the samples were stored in a climatic chamber at 20 °C and 55% relative humidity. In the first 10 days, the length change measurements were made every day. After that, the shrinkage was monitored periodically up to 28 days of drying.

### 3.4. Determination of Photocatalytic Activity

The photocatalytic properties of modified gypsum plasters toward air purification were estimated during NO<sub>x</sub> degradation. The detailed parameters of the process and the scheme of NO<sub>x</sub> installation were depicted in our previous works [41,42]. Briefly, in each test, the four gypsum plates were placed in the center of a quartz cylindrical reactor with dimensions of  $\varnothing \times H = 9 \times 32$  cm, which was surrounded by four UV lamps ( $4 \times 22$  W, Philips) with the cumulative radiation intensity of 100 W/m<sup>2</sup> UV and 4 W/m<sup>2</sup> vis. The emission spectra of these lamps is presented in Figure 5. The left side of the reactor was connected to a NO gas source, while the right side was connected to an NO<sub>x</sub> analyzer (T200, Teledyne Advanced Pollution Instrumentation, USA). The starting NO gas was in advance diluted by a humidified synthetic air in a ratio of 1:1 to the target initial concentration of about 1 ppm and flowed through the reactor with the flow rate of 500 cm<sup>3</sup>/min. The operation principle of the NO<sub>x</sub> analyzer is based on the chemiluminescence. The NO and NO<sub>2</sub> concentrations were continuously measured in the outlet of the reactor and registered every 1 min. The temperature of the processes was maintained at 22 °C by using a thermostatic chamber.

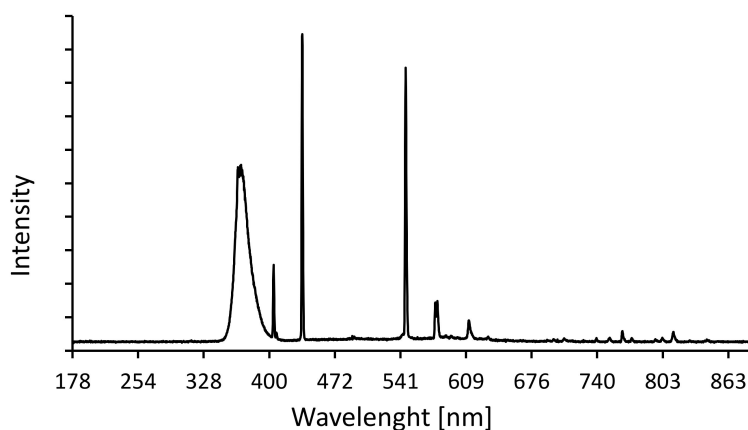


**Figure 5.** Emission spectra four UV lamps ( $4 \times 22$ W, Philips) with the cumulative radiation intensity of 100 W/m<sup>2</sup> UV and 4 W/m<sup>2</sup> vis.

At the beginning of the process, the gas flowed in the dark condition in order to fully eliminate the existing air in the reactor as well as to create a gas–solid adsorption–desorption equilibrium (about 35 min). Then, the UV lamps were turned on for 30 min, and the proper photocatalytic reactions were activated.

The photocatalytic performance was evaluated in terms of two indicators referring to  $\text{NO}_x$  concentration. Namely, the ‘ $\text{NO}_x$  total removal’ shows the amount of  $\text{NO}_x$  in  $\mu\text{g}$  that can be removed per square centimeter per hour, whereas the ‘rate of  $\text{NO}_x$  degradation’ is a dimensionless measure of  $\text{NO}_x$  removal expressed in percentage that considers the real surface area of the specimens.

The self-cleaning properties of modified gypsum plasters were estimated during organic dyes degradation: Reactive Orange 20 and Malachite Green. Gypsum plates were dipped into 4  $\text{cm}^3$  of RO or MG aqueous solution at concentration of 100  $\text{mg}/\text{dm}^3$  for 0.5 h. The imbued samples were removed from dye solution and dried at 40 °C for 24 h. The photocatalytic tests were conducted under UV irradiation ( $6 \times 15$  W, Cleo, Berlin, Germany) with the cumulative radiation intensity of 83.4  $\text{W}/\text{m}^2$  UV and 100  $\text{W}/\text{m}^2$  vis. The emission spectra of these lamps is presented in Figure 6. The total time of irradiation amounted to 40 h, whereas the polluted samples were measured every 5 or 10 h. The distance between the stained gypsum samples and the source of UV irradiation was 25 cm. The colorimetric method was used to determine the dyes’ degradation rate (RE).

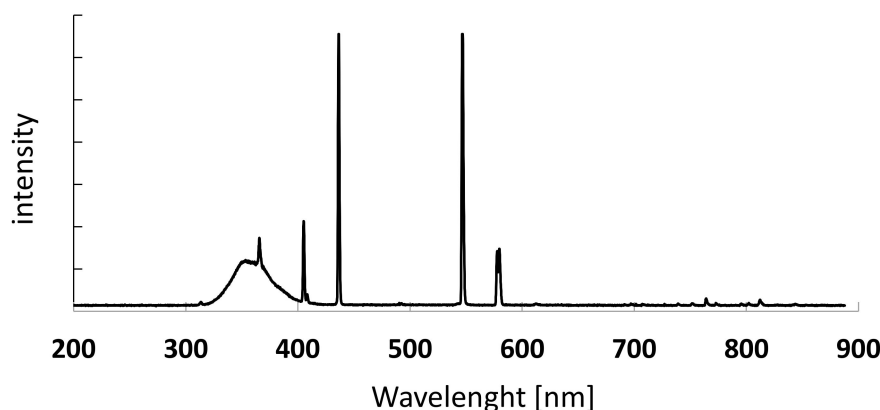


**Figure 6.** Emission spectra of six UV lamps ( $6 \times 15$ W, Cleo, Berlin, Germany) with the cumulative radiation intensity of 83.4  $\text{W}/\text{m}^2$  UV and 100  $\text{W}/\text{m}^2$  vis.

The colorimeter CP-21 (tri-color) allowed registering the color changes on the surfaces of the samples. In the method, colors are expressed in the CIELAB system (Commission Internationale de l’Eclairage), and hence the color space is defined by three different chromatic coordinates (L, a, and b) [43]. The procedure of colorimetric calculations was carried out on the basis of the literature report [44], and it was detailed described in our previous work [11].

#### 4. Conclusions

Commercial gypsum plaster modified with 1 wt % of  $\text{TiO}_2/\text{N}$  photocatalyst, 0.01–0.2 wt % of polycarboxylic superplasticizer, and an optional with 0.3 wt % of glass fiber was analyzed in detail regarding the consistency, setting time, mechanical strength, shrinkage, and photocatalytic properties. Based on the results from this study, the following conclusions can be drawn:

- A higher density of gypsum mortars as a result of 1 wt % of  $\text{TiO}_2/\text{N}$  photocatalyst presence might be regulated to normal consistency by 0.01 wt % of polycarboxylic superplasticizer. Moreover, the water content in the photocatalytic mortar can be reduced about 12% by 0.2 wt % of the SP.
- The setting time was shortened through the catalytic action of  $\text{TiO}_2/\text{N}$  in the hydration process and the facilitation of hydration by side chains of SP molecules as well as the lower water content to evaporation.

- The decrease of mechanical strength, which was observed after photocatalyst addition into gypsum plaster, was eliminated by SP. Precisely, a 12% reduction of water in the photocatalytic plaster, which was possible thanks to using the SP, involved prominent increases in the flexural and compressive strength of 77% and 68%, respectively, which correspond to 42% and 32% higher strengths in relation to the reference gypsum plaster. The additional glass fiber in the modified matrix enhanced the mechanical strength by several more percentages. The glass fiber should be accompanied by a superplasticizer to achieve the proper reinforcing action.
- The application of additional components such as SP and fiber reinforcement in a photocatalytic gypsum matrix might compensate for the mechanical changes induced by the connected photocatalyst particles, especially their high water demand and the changes of the pores' distribution in gypsum material.
- Shrinkage reduction is mainly associated with photocatalyst presence and lower water content except for the obvious significance of curing conditions such as temperature and moisture level. The influence of superplasticizer molecules and glass fiber on shrinkage behavior was negligible.
- The modified materials can support the elimination of NO<sub>x</sub> from the air. The photocatalytic activity of photocatalytic gypsum plaster was maintained on the level of 30%, regardless of SP or glass fiber presence.
- The self-cleaning properties of gypsum material were gradually improved by (1) a modified photocatalyst (photocatalytic action), (2) to some extent by superplasticizer molecules due to limited agglomeration and the more accessible active photocatalyst surface, and (3) nearly two times by glass fiber due to the transportation of irradiation to deeper parts of the gypsum materials. The synergistic effect of the three components in a gypsum matrix during self-cleaning phenomenon was confirmed.

Prepared gypsum mixtures have adequate technical parameters and photocatalytic properties that allow classifying them as multi-functional gypsum plasters.

**Author Contributions:** Conceptualization, K.Z. and M.J.; methodology, K.Z., M.J. and A.C.; formal analysis, K.Z. and M.J.; investigation, K.Z.; writing—original draft preparation, K.Z.; writing—review and editing, K.Z. and M.J.; supervision, M.J.; funding acquisition, M.K. All authors have read and agreed to the published version of the manuscript.

**Funding:** This research received no external funding.

**Conflicts of Interest:** The authors declare no conflict of interest.

## References

1. Jimenez-Relinque, E.; Castellote, M. Quick assessment of the photocatalytic activity of TiO<sub>2</sub> construction materials by nitroblue tetrazolium (NBT) ink. *Constr. Build. Mater.* **2019**, *214*, 1–8. [[CrossRef](#)]
2. Binas, V.; Papadaki, D.; Maggos, T.; Katsanaki, A.; Kiriakidis, G. Study of innovative photocatalytic cement based coatings: The effect of supporting materials. *Constr. Build. Mater.* **2018**, *168*, 923–930. [[CrossRef](#)]
3. Su, B.; Zhong, M.; Han, L.; Wei, M.; Liu, Y.; Yang, H.; Lei, Z. Eco-friendly preparation of hierarchically self-assembly porous ZnO nanosheets for enhanced photocatalytic performance. *Mater. Res. Bull.* **2020**, *124*, 110777–110781. [[CrossRef](#)]
4. Shafaei, D.; Yang, S.; Berlouis, L.; Minto, J. Multiscale pore structure analysis of nano titanium dioxide cement mortar composite. *Mater. Today Commun.* **2020**, *22*, 100779–100788. [[CrossRef](#)]
5. Makul, N. Modern sustainable cement and concrete composites: Review of current status, challenges and guidelines. *Sustain. Mater. Technol.* **2020**, *25*, e00155–e00169. [[CrossRef](#)]
6. Demeestere, K.; Dewful, J.; De Witte, B.; Beeldens, A.; Van Langenhove, H. Heterogeneous photocatalytic removal of toluene from air on building materials enriched with TiO<sub>2</sub>. *Build. Environ.* **2008**, *43*, 406–414. [[CrossRef](#)]
7. Chen, J.; Qiu, F.; Xu, W.; Cao, S.; Zhu, H. Recent progress in enhancing photocatalytic efficiency of TiO<sub>2</sub>-based materials. *Appl. Catal. A Gen.* **2015**, *495*, 131–140. [[CrossRef](#)]

8. Yang, Y.; Ji, T.; Su, W.; Yang, B.; Zhang, Y.; Yang, Z. Photocatalytic NO<sub>x</sub> abatement and self-cleaning performance of cementitious composites with g-C<sub>3</sub>N<sub>4</sub> nanosheets under visible light. *Constr. Build. Mater.* **2019**, *225*, 120–131. [[CrossRef](#)]
9. García Calvo, J.L.; Carballosa, P.; Castillo, A.; Revuelta, D.; Gutiérrez, J.P.; Castellote, M. Expansive concretes with photocatalytic activity for pavements: Enhanced performance and modifications of the expansive hydrates composition. *Constr. Build. Mater.* **2019**, *218*, 394–403. [[CrossRef](#)]
10. Li, H.; Ding, S.; Zhang, L.; Ouyang, J.; Han, B. Effects of particle size, crystal phase and surface treatment of nano-TiO<sub>2</sub> on the rheological parameters of cement paste. *Constr. Build. Mater.* **2020**, *239*, 117897–117906. [[CrossRef](#)]
11. Zając, K.; Janus, M.; Morawski, A.W. Improved self-cleaning properties of photocatalytic gypsum plaster enriched with glass fiber. *Materials* **2019**, *12*, 357. [[CrossRef](#)] [[PubMed](#)]
12. Pelaez, M.; Nolan, N.T.; Pillai, S.C.; Seery, M.K.; Falaras, P.; Kontos, A.G.; Dunlop, P.; Hamilton, J.; Byrne, J.; O’Shea, K.; et al. A review on the visible light active titanium dioxide photocatalysts for environmental applications. *Appl. Catal. B Environ.* **2012**, *125*, 331–349. [[CrossRef](#)]
13. Wang, W.; Tadó, M.O.; Shao, Z. Nitrogen – doped simple and complex oxides for photocatalysis: A review. *Prog. Mater. Sci.* **2018**, *92*, 33–63. [[CrossRef](#)]
14. Noaman, A.T.; Abed, M.S.; Hamead, A.A.A. Production of polycarboxylate-ether superplasticizer (PCE) coated sand with modified hardened properties in cement mortar. *Constr. Build. Mater.* **2020**, *245*, 118442–118450. [[CrossRef](#)]
15. Ma, B.; Qi, H.; Tan, H.; Su, Y.; Li, X.; Liu, X.; Li, C.; Zhang, T. Effect of aliphatic-based superplasticizer on rheological performance of cement paste plasticized by polycarboxylate superplasticizer. *Constr. Build. Mater.* **2020**, *233*, 117181–117189. [[CrossRef](#)]
16. Haruna, S.; Fall, M. Time- and temperature- dependent rheological properties of cemented paste backfill that contains superplasticizer. *Powder Technol.* **2020**, *360*, 731–740. [[CrossRef](#)]
17. Vo, M.L.; Plank, J. Dispersing effectiveness of a phosphated polycarboxylate in  $\alpha$ - and  $\beta$ -calcium sulfate hemihydrate systems. *Constr. Build. Mater.* **2020**, *237*, 117731–117741. [[CrossRef](#)]
18. Lin, X.; Liao, B.; Zhang, J.; Li, S.; Huang, J.; Pang, H. Synthesis and characterization of high –performance cross-linked polycarboxylate superplasticizers. *Constr. Build. Mater.* **2019**, *210*, 162–171. [[CrossRef](#)]
19. Yang, L.; Yilmaz, E.; Li, J.; Liu, H.; Jiang, H. Effect of superplasticizer type and dosage on fluidity and strength behavior of cement tailings backfill with different solid contents. *Constr. Build. Mater.* **2018**, *187*, 290–298. [[CrossRef](#)]
20. Tan, H.; Deng, X.; Gu, B.; Ma, B.; Luo, S.; Zhi, Z.; Guo, Y.; Zou, F. Effect of borax and sodium tripolyphosphate on fluidity of gypsum paste plasticized by polycarboxylate superplasticizer. *Constr. Build. Mater.* **2018**, *176*, 394–402. [[CrossRef](#)]
21. Peng, J.; Qu, J.; Zhang, J.; Chen, M.; Wan, T. Adsorption characteristics of water—Reducing agents on gypsum surface and its effect on the rheology of gypsum plaster. *Cement Concrete Res.* **2005**, *35*, 527–531. [[CrossRef](#)]
22. Guan, B.; Ye, Q.; Zhang, J.; Lou, W.; Wu, Z. Interaction between  $\alpha$ —calcium sulfate hemihydrate and superplasticizer from the point of adsorption characteristics, hydration and hardening process. *Cement Concrete Res.* **2010**, *40*, 253–259. [[CrossRef](#)]
23. Pundir, A.; Garg, M.; Singh, R. Evaluation of properties of gypsum plaster—Superplasticizer blends of improved performance. *J. Build. Eng.* **2015**, *4*, 223–230. [[CrossRef](#)]
24. Sakthieswaran, N.; Sophia, M. Effect of superplasticizers on the properties of latex modified gypsum plaster. *Constr. Build. Mater.* **2018**, *179*, 675–691. [[CrossRef](#)]
25. Zając, K.; Rucińska, T.; Morawski, A.; Janus, M. Photocatalytic gypsum plasters – studies of air cleaning properties and selected technical parameters. *Cem. WapnoBeton* **2019**, *1*, 10–20.
26. Kondratieva, N.; Barre, M.; Goutenoire, F.; Sanytsky, M.; Rousseau, A. Effect of additives SiC on the hydration and the crystallization processes of gypsum. *Constr. Build. Mater.* **2020**, *235*, 117479–117488. [[CrossRef](#)]
27. Moghadam, H.A.; Mirzaei, A. Comparing the effects of a retarder and accelerator on properties of gypsum building plaster. *J. Build. Eng.* **2020**, *28*, 101075–101082. [[CrossRef](#)]
28. Chen, J.; Kou, S.C.; Poon, C.S. Hydration and properties of nano-TiO<sub>2</sub> blended cement composites. *Cement Concrete Comp.* **2012**, *34*, 642–649. [[CrossRef](#)]

29. Lucas, S.S.; Ferreira, V.M.; Barroso de Aguiar, J.L. Incorporation of titanium dioxide nanoparticles in mortars—Influence of microstructure in the hardened state properties and photocatalytic activity. *Cement Concrete Res.* **2013**, *43*, 112–120. [[CrossRef](#)]
30. Wu, H.-C.; Xia, Y.-M.; Hu, X.-Y.; Liu, X. Improvement on mechanical strength and water absorption of gypsum modeling material with synthetic polymers. *Ceram. Int.* **2014**, *40*, 14899–14906. [[CrossRef](#)]
31. Zhang, G.; Li, G.; Li, Y. Effects of superplasticizers and retarders on the fluidity and strength of sulphoaluminate cement. *Constr. Build. Mater.* **2016**, *126*, 44–54. [[CrossRef](#)]
32. Huang, W.-H. Improving the properties of cement-fly ash grout using fiber and superplasticizer. *Cement Concrete Res.* **2001**, *31*, 1033–1041. [[CrossRef](#)]
33. Farzadnia, N.; Noorvand, H.; Yasin, A.M.; Aziz, F.N.A. The effect of nano silica on short term drying shrinkage of POFA cement mortars. *Constr. Build. Mater.* **2015**, *95*, 636–646. [[CrossRef](#)]
34. Sonebi, M.; García-Taengua, E.; Hossain, K.M.A.; Khatib, J.; Lachemi, M. Effect of nanosilica addition on the fresh properties and shrinkage of mortars with fly ash and superplasticizer. *Constr. Build. Mater.* **2015**, *84*, 269–276. [[CrossRef](#)]
35. Alsayed, S.H. Influence of superplasticizer, plasticizer, and silica fume on the drying shrinkage of high-strength concrete subjected to hot-drying field conditions. *Cement Concrete Res.* **1998**, *28*, 1405–1415. [[CrossRef](#)]
36. Hwang, C.-L.; Tran, V.-A.; Hong, J.-W.; Hsien, Y.-C. Effects of short coconut fiber on the mechanical properties, plastic cracking behavior, and impact resistance of cementitious composites. *Constr. Build. Mater.* **2016**, *127*, 984–992. [[CrossRef](#)]
37. Mohammed, B.S.; Khed, V.C.; Liew, M.S. Optimization of hybrid fibres in engineering cementitious composites. *Constr. Build. Mater.* **2018**, *190*, 24–37. [[CrossRef](#)]
38. Nguyen, C.H.; Fu, C.C.; Juang, R.S. Degradation of methylene blue and methyl orange by palladium-doped TiO<sub>2</sub> photocatalysis for water reuse: Efficiency and degradation pathways. *J. Clean. Prod.* **2018**, *202*, 413–427. [[CrossRef](#)]
39. Bubacz, K.; Choina, J.; Dolat, D.; Borowiak-Paleń, E.; Moszyński, D.; Morawski, A.W. Studies on nitrogen modified TiO<sub>2</sub> photocatalyst prepared in different conditions. *Mater. Res. Bull.* **2010**, *45*, 1085–1091. [[CrossRef](#)]
40. Janus, M.; Mađraszewski, S.; Zając, K.; Kusiak-Nejman, E.; Morawski, A.W.; Stephan, D. Photocatalytic activity and mechanical properties of cements modified with TiO<sub>2</sub>/N. *Materials* **2019**, *12*, 3756. [[CrossRef](#)]
41. Zając, K.; Janus, M.; Kuźmiński, K.; Morawski, A.W. Preparation of gypsum building materials with photocatalytic properties. A strong emphasis on waste gypsum from flue gas desulfurization. *Przem. Chem.* **2016**, *95*, 2222–2226.
42. Janus, M.; Zając, K.; Ehm, C.; Stephan, D. Fast method for testing the photocatalytic performance of modified gypsum. *Catalysts* **2019**, *9*, 693. [[CrossRef](#)]
43. Munafò, P.; Goffredo, G.B.; Quagliarini, E. TiO<sub>2</sub>-based nanocoatings for preserving architectural stone surfaces: An overview. *Constr. Build. Mater.* **2015**, *84*, 201–218. [[CrossRef](#)]
44. Graziani, L.; Quagliarini, E.; D’Orazio, M. The role of roughness and porosity on the self-cleaning and anti-biofouling efficiency of TiO<sub>2</sub>-Cu and TiO<sub>2</sub>-Ag nanocoatings applied on fired bricks. *Constr. Build. Mater.* **2016**, *129*, 116–124. [[CrossRef](#)]

